



# Monolayers of pigment-protein complexes on a bare gold electrode: Orientation controlled deposition and comparison of electron transfer rate for two configurations

Muhammad Kamran<sup>a,\*</sup>, Namik Akkilic<sup>a,b</sup>, Jinghui Luo<sup>c</sup>, Azhar Z. Abbasi<sup>d</sup>

<sup>a</sup> Leiden Institute of Physics, Leiden University, Niels Bohrweg 2, 2333CA Leiden, The Netherlands

<sup>b</sup> Membrane Science and Technology, Mesa+ Institute for Nanotechnology, University of Twente, P.O. Box 217, 7500 AE Enschede, The Netherlands

<sup>c</sup> Leiden Institute of Chemistry, Leiden University, Einsteinweg 55, 2333CC Leiden, The Netherlands

<sup>d</sup> Department of Pharmaceutical Sciences, Leslie L. Dan Faculty of Pharmacy, University of Toronto, Toronto, Ontario M5S 1A5, Canada

## ARTICLE INFO

### Article history:

Received 8 November 2014

Received in revised form

10 January 2015

Accepted 26 January 2015

Available online 7 February 2015

### Keywords:

Reaction center-light harvesting 1 complex

Electron transfer

Langmuir Blodgett deposition

*I*–*V* spectroscopy

Photocurrent

Gold electrode

## ABSTRACT

Photosynthetic protein complexes are efficient in light energy absorption, excitation transfer, and subsequent electron transfer. These complexes have the potential to be exploited as circuit elements for various bio-hybrid devices, ranging from biosensors to solar cells. In this report, we characterized a bioelectronic composite fabricated by interfacing reaction center-light harvesting 1 (RC-LH1) complex with an un-functionalized gold surface in defined orientation. The orientation of RC-LH1 complex was controlled by using Langmuir–Blodgett deposition technique: RC-LH1 complexes were attached to the electrode facing either their primary donor or the acceptor sides by “forward” or “reverse” dipping, respectively. Photochromic microscopy was utilized to confirm the integrity of the protein complexes and their orientation. The electrical transport of protein complexes coupled to gold electrode was studied by using conductive atomic force microscopy (C-AFM). Two distinct current–voltage (*I*–*V*) curves were observed for two different deposition schemes, indicating opposite orientations of RC-LH1 complexes on the electrode. *I*–*V* spectroscopy was also carried out under light illumination, the magnitude of current was increased by the light illumination and the asymmetry of the curves was more pronounced. These results show that, RC-LH1 complexes attached to the electrode with primary donor side facing the electrode exhibit much faster electron transfer compared to opposite orientation.

© 2015 Elsevier B.V. All rights reserved.

## 1. Introduction

The interfacing of biomolecules to electrodes, such as metal electrodes, is a central issue in bio nanoscience. Typically, a bioelectronic device, for example, a sensor or a biofuel cell, consists of an assembly of redox active proteins on a conducting electrode such that their bio catalytic activity can be transformed into a measurable output signal by electronic transduction (Willner and Katz, 2000). Direct coupling of the bioactive redox enzyme or protein to an electrode offers important advantages from a technological point of view in terms of efficiency, reactivity, specificity, selectivity and sensitivity. Hence, biomolecular components are being explored as building blocks for materials and devices for a variety of purposes, at a rapidly increasing rate. This development is gaining momentum because it is at the core of bionanotechnology

which is a major focus of current research across the globe. Significant research activities in this field are aimed at the integration of macromolecules of biological origin with electronic circuits, based on the assumption that this will ultimately provide the elementary basis for the design of novel bioelectronic devices (Katz and Willner, 2003). Such devices may incorporate redox-active proteins and enzymes, which in particular, have a natural propensity for interaction by exchanging their electrons (Akkilic et al., 2014; Willner et al., 2006). Recent applications of photosensitive enzymes and proteins, for example, have shown their potential in solar energy conversion (Das et al., 2004; Nguyen and Bruce, 2014), optical memories (Kim et al., 2010), optical bioswitches (Liljeroth, 2012), biosensors (Swainsbury et al., 2014), and biological actinometers (Liu et al., 1992). The scope of interfacing can be extended to three dimensions to enhance functional sensitivity and selectivity.

Due to high internal quantum efficiency, photosynthetic pigment protein complexes are very attractive for photovoltaic applications (Yehezkeili et al., 2014, 2012). In recent years several attempts have been made to construct the functional devices

\* Corresponding author.

E-mail addresses: [Kamran@physics.leidenuniv.nl](mailto:Kamran@physics.leidenuniv.nl), [kamranphy81@gmail.com](mailto:kamranphy81@gmail.com) (M. Kamran).

based on biological entities extracted from photosynthetic systems (Kothe et al., 2014; Mershin et al., 2012; Mirvakili et al., 2014; Tan et al., 2012a, 2012b, 2013). Immobilized protein complexes on conducting surfaces retain their function of light absorption and energy transduction but the quantum efficiency of these devices is quite low.

Photosynthetic reaction center (RC) has been intensively studied as a model system to understand the basis of light absorption and energy transduction. Light-induced charge separation in photosynthetic RC is unidirectional; therefore the performance of any device based on these complexes is strongly dependent on orientation of the complexes on the electrode. The optimum orientation of the protein complexes is generally achieved by adsorbing the desired molecules on electrode, which are pre-modified with a self-assembled monolayer (SAM) of organic molecules, or specifically, binding the genetically modified complexes with the electrode (Das et al., 2004; Kondo et al., 2012; Reiss et al., 2007). In this manner, monolayers of proteins with defined orientation is achieved however, the main disadvantage of these methods is that the electron transfer drops drastically due to increase in tunneling distance introduced by the SAM or linker molecule.

Langmuir–Blodgett (LB) deposition is a well-known technique to assemble self-organized molecular monolayer at water–air interface, which is subsequently transferred onto a solid support (Yan et al., 2012). The most striking feature of LB technique is the control of the thickness and orientation of the deposited layers. This method has been extensively used to deposit mono (multi) layers of the various kinds of molecules, including protein complexes onto a variety of substrates with precise control (Alegria and Dutton, 1991a, 1991b; Facci et al., 1998; Fang et al., 1995; Kuda et al., 1992; Talham et al., 2008; Tredgold, 1985; Ueno et al., 1998; Uphaus et al., 1997; Yan et al., 2012; Yasuda et al., 1997, 1994, 1998; Zhao et al., 1992).

Herein, reaction center–light harvesting 1 (RC–LH1) complex from *Rhodospseudomonas* (*Rps.*) *acidophila* was attached to semi-transparent (12 nm thick) gold electrodes using Langmuir–Blodgett deposition method. This particular protein complex is interesting to study because it has been shown to be superior in terms of connectivity in terms of high photocurrent generation thus to produce bioelectronic devices (den Hollander et al., 2008; Kamran et al., 2014). Herein, we have employed two different dipping strategies: (1) dipping the slide into the surface assembled monolayer (“forward dip”), (2) Pulling the gold coated slide out of the surface assembled monolayer (“reverse dip”). Direction of light-induced current indicates the orientation of the complexes on conductive electrode, which is corroborated by current–voltage (*I*–*V*) curves of the complexes acquired using conductive atomic force microscopy (C-AFM). *I*–*V* curves acquired under light illumination showed enhancement in the magnitude of the current, providing an evidence of light induced electron transfer in dried LB films. The enhancement of the current under light illumination was more pronounced for RC–LH1 attached to the electrode via primary donor side compared to the opposite orientation. We show that LB films of RC–LH1 complexes retain their function of light absorption and facilitate electron transfer on gold electrodes both in buffer and dried form. The size of the RC–LH1 complex is also estimated from compression curve which is in line with the dimensions of the complex based on its crystal structure.

## 2. Materials and methods

### 2.1. Materials

Cytochrome C (cyt c) from horse heart and 2, 3-dimethoxy-5-

methyl-*p*-benzoquinone (ubiquinone-0, Q-0), both were purchased from Sigma and used without further purification.

### 2.2. RC–LH1 isolation

RC–LH1 complexes were isolated from *Rps. acidophila* by using protocol from Cogdell et al. (Cogdell et al., 1983) and suspended in buffer (10 mM Tris, pH 8), supplemented with 0.1% Laurdimethylamine-N-oxide (LDAO) and 1 mM EDTA.

### 2.3. Langmuir Blodgett film

Monolayer of RC–LH1 complexes was prepared using KSV Nima trough (KSV instruments Co., Helsinki, Finland). The sub-phase of the LB trough contained only distilled water, RC–LH1 complexes (1 mg/ml) were spread over the water surface and allowed to settle for 15–20 minutes. The monolayer was compressed between the barriers of the trough and subsequently transferred onto a gold electrode. Two types of films were deposited on bare gold electrode: (i) forward-dipped film was fabricated by dipping the gold-coated glass coverslip into the surface assembled monolayer with a speed of 2 mm/min and pulling out with a speed of 20 mm/min. (ii) The reverse-dipped film was deposited by pulling out the gold-coated coverslip with the speed of 2 mm/min. The surface pressure was kept constant during the dipping process.

### 2.4. Preparation of gold electrode

Working electrodes were prepared by coating MENZEL GLÄSER Nr. 1 glass cover slips (Gerhard Menzel GmbH, Germany) with a thin layer of gold (12 nm). The glass cover slips were first cleaned with acetone, then with methanol for 1 h, then washed with distilled water and dried under the stream of nitrogen. The dried cover slips were placed in ozone cleaner for one hour (PR-100, UV Ozone Photoreactor, UVP). A Magnetron sputtering system (ATC 1800-F, AJA Corporation) was utilized to deposit a thin layer of gold onto clean glass coverslips. An additional layer of 1–2 nm of molybdenum–germanium (MoGe) was sputtered on glass coverslips prior to gold sputtering to increase the adhesion between gold and glass. Thin layer of MoGe was deposited at a rate of 1.32 nm/min under 10 mtorr Argon environment, whereas gold deposition was carried out at a rate of 9.06 nm/min under Argon and oxygen environment (10 mTorr Argon and 1mTorr Oxygen). The root mean square roughness of the deposited films was 2–3 Å (Akkilic et al., 2014; Salverda et al., 2010).

### 2.5. Conductive atomic force microscopy

Current–voltage (*I*–*V*) curves of LB monolayers were acquired by C-AFM under ambient condition using commercial atomic force microscope, equipped with an E-Scanner and a current amplifier (AFM, Nanoscope IIIa, Veeco, USA). The tunneling junction was fabricated by sandwiching the monolayer of RC–LH1 complexes between gold electrode and AFM tip. In order to meet the requirements of the experiments, standard silicon nitride cantilevers with spring constant of 2 N/m and resonant frequency of 75 kHz were coated with a thin layer of gold using magnetron sputtering system. RC–LH1 complexes were located by imaging in tapping mode; the instrument was switched to contact mode after placing the AFM tip at desired location. A potential ramp was applied between the two electrodes and resulting current was measured to construct *I*–*V* curves. *I*–*V* curves for both forward- and reverse-dipped films were recorded by varying contact force and light conditions. *I*–*V* curves under light illumination were acquired by shining the sample with a light-emitting diode (LED) of central wavelength of 880 nm and bandwidth of 50 nm.

## 2.6. Photochronoamperometry

After depositing LB film of RC-LH1 complexes, the gold-coated glass coverslip was fixed as the base of a measuring cell containing buffer (10 mM Tris HCl, pH 8). Light-induced currents were measured under ambient conditions using potentiostat (Metrohm-Autolab PGSTAT 128 N), integrated with conventional three electrodes setup, a gold-coated glass coverslip as working electrode, a saturated calomel electrode (SCE) as reference electrode, and platinum wire serving as the counter electrode. Light illumination (by a light-emitting diode centered at 880 nm, with a band width of 50 nm) was provided from the bottom of the cell, through the gold-coated glass coverslip. Quinones and cytochrome c were used as redox mediators in the buffer solution. Light illumination intensity was 23 mW/cm<sup>2</sup> for all the experiments, measured by the power meter. A computer controlled shutter was placed between the light source and working electrode to turn the light illumination on/off. A picture of the experimental setup is provided in Supporting Information (Fig. S2).

## 2.7. Absorption spectra of Langmuir Blodgett films

Absorption spectra of LB films deposited on gold electrode were acquired using a fiber-coupled spectrometer (QE 6500, Ocean Optics Inc.), equipped with a halogen light source.

## 3. Results and discussion

### 3.1. Monolayer formation and transfer onto electrode

After spreading detergent solubilized RC-LH1 on air-water interface, the film was compressed and pressure-area isotherm was recorded. The RC-LH1 complexes arranged themselves on water surface with their more hydrophilic part facing the water as shown in Fig. 1A. RC complexes have, previously, been employed at water-air interface with slightly more hydrophilic side towards water and less hydrophilic side hanging in air (Yasuda et al., 1992, 1994; Zaitsev et al., 1992). The collapse pressure was found to be 55 mN/m. The surface pressure-area isotherm shows (Fig. S1) two distinct regions corresponding to two different packing density states: liquid and solid. The gas phase may not be visible because of

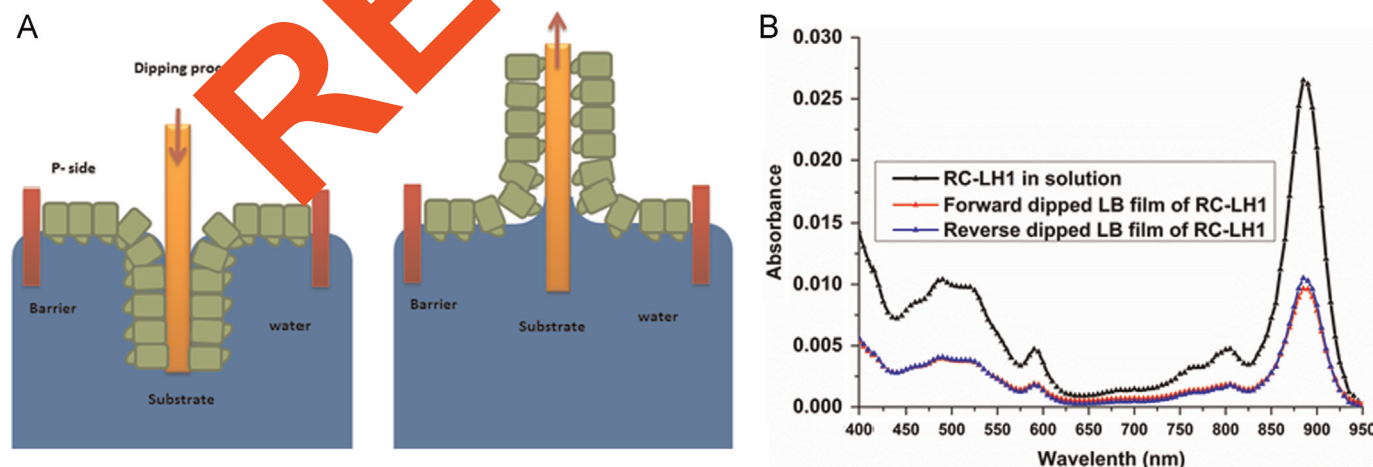
large area of RC-LH1 molecule. In order to avoid squeezed state, the deposition pressure was selected at the beginning of the solid state region. The limiting area for RC-LH1 was evaluated to be  $110 \pm 10 \text{ nm}^2$  / RC-LH1 complex, which is comparable to size ( $11 \times 11 \text{ nm}^2$ ) of the complex calculated from x-rays crystallography (Roszak et al., 2003). Surface assembled monolayer of RC-LH1 complexes was transferred onto a freshly sputtered gold surface for further characterization. Morphology of the LB films deposited on gold electrode was monitored by AFM imaging under ambient conditions. AFM images show similar surface coverage of both kinds of films (Figs. S5 and S6).

Fig. 1B shows that the absorption spectra of forward- and reverse-dipped LB films have similar characteristic peaks to that of absorption spectrum in solution. All the major peaks associated with RC (800 nm), LH1 ring (885 nm) and carotenoids (400–500 nm) are intact in the spectra from both kinds of films. It may lead us to a conclusion that LB deposition does not induce considerable structural deformation during the deposition process. Similar surface coverage is also depicted by the absorption spectra of forward- and reverse-dipped LB films.

### 3.2. Electrochemical characterization of LB films

Bacterial reaction center complex generates charge separation at primary donor site, so called special pair by absorbing light energy. Initial charge separation leads to a transmembrane electron transfer, assisted by its co-factors. Transmembrane electron transfer is coupled to a proton gradient across the membrane; the special pair is reduced by cytochrome c to complete cyclic electron transfer. This charge separation at special pair can be transferred to an electrode by interfacing the RC or RC-LH1 complex with a metal electrode. We have used Q-0 and Cyt c in the electrolyte to replicate the cyclic electron transfer, for RC-LH1 deposited on electrode.

Photocurrent measurements were carried out in a home built electrochemical cell, which was designed to incorporate a gold-coated (12 nm) glass coverslip as a working electrode (Fig. 2A and S2). After depositing LB film, the gold-coated coverslip was fixed in an electrochemical cell where a reference and a counter electrode were also inserted in the electrolyte (10 mM Tris HCl, pH 8). Potential was set to  $-100 \text{ mV}$  vs SCE. Upon turning on the light illumination, cathodic current was recorded in presence of charge



**Fig. 1.** (A) Schematic representation of the Langmuir-Blodgett deposition method for defined orientation of reaction center-light harvesting 1 (RC-LH1) complex. Two different strategies are shown in the figure, representing forward-dipped (left panel) and reverse-dipped (right panel) deposition procedure. Surface assembled monolayer of RC-LH1 complexes on water air interface is compressed with the barriers to a certain pressure; subsequently a gold coated slide is dipped into or pulled out of the monolayer, depending on the requirement of the experiment, keeping the surface pressure constant. (B) Absorption spectrum of RC-LH1 complexes in solution and absorption spectra of forward- and reverse-dipped LB films. Absorption spectra of LB films are measured using fiber-coupled spectrometer equipped with a halogen light source. Overlaid spectra are shown for comparison.



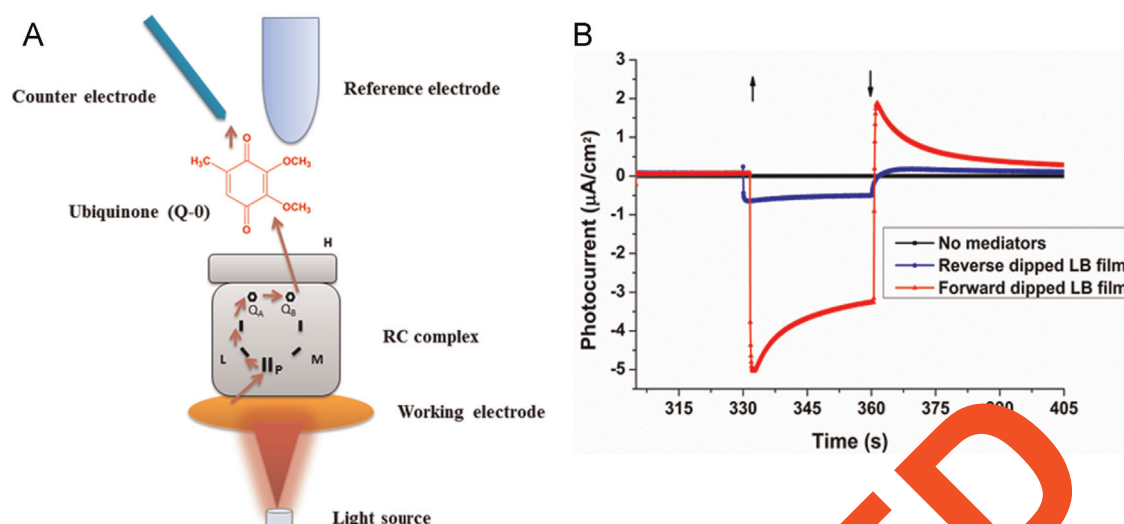


**Fig. 2.** (A) Schematic representation of the setup used for light induced current measurements. RC-LH1 complexes are immobilized on a gold electrode, serving as a working electrode. Reference (saturated calomel) and counter (platinum wire) electrodes are inserted from the top. Light illumination is provided from the bottom of the electrochemical cell. RC complex has three types of peptide represented by L, M and H in the figure. Electron transfer in RC is initiated by charge separation at dimer of bacteriochlorophyll, called special pair (P) which ends up at Quinone B ( $Q_B$ ) after multiple tunneling steps involving bacteriochlorophyll, bacteriopheophytin and Quinone A ( $Q_A$ ). Pathway of the electron is indicated by the arrows in the figure. (B) Photocurrents recorded by forward-dipped LB film (red triangles), reverse-dipped LB film (blue circles), and LB film without any mediator present in the solution. The arrows in the figure show the switching of the light (arrow pointing upwards) and off (arrow pointing downwards). The applied potential for all the experiments was  $-100$  mV (vs. SCE). Light illumination was provided by an LED ( $23$  mW/cm $^2$ ). Quinones ( $100$   $\mu$ M) and Cyt c ( $20$   $\mu$ M) are used as mediators for both types of films. (For interpretation of the references to color in this figure legend, the reader is referred to the web version of this article.)

carriers ( $100$   $\mu$ M Q-0 and  $20$   $\mu$ M Cyt c). Omitting both the charge carriers from the electrolyte, no photocurrent was observed (Fig. 2B, black line). Despite similar surface coverage (depicted by similar absorption spectra in Fig. 1B) and other experimental conditions (mediator's concentration and applied potential), the magnitude of photocurrent for forward-dipped LB was found to be  $5$  times higher than that of reverse-dipped film (Fig. 2B). The observation of cathodic current in similar experiments is attributed to the flow of electrons from working electrode to special pair of RC complex (den Hollander et al., 2011; Lebedev et al., 2006; Swainson et al., 2014; Trammell et al., 2006).

By using only  $100$   $\mu$ M Q-0 as mediator, photocurrent of  $1100 \pm 8$  nA/cm $^2$  for forward-dipped and  $105 \pm 5$  nA/cm $^2$  for reverse-dipped film was recorded. The magnitude of photocurrent is enhanced significantly ( $5 \pm 0.5$  nA/cm $^2$  for forward-dipped and  $500 \pm 9$  nA/cm $^2$  for reverse-dipped film) by supplementing the electrolyte with  $20$   $\mu$ M cyt c. The enhancement of photocurrent by addition of cyt c is attributed to the wiring effect provided by cyt c between primary donor side of RC complex and the working electrode (Lebedev et al., 2006). The magnitude of the photocurrent was further increased by increasing the concentration of Q-0 and cyt c. At a certain concentration of the mediators ( $1600$   $\mu$ M and  $320$   $\mu$ M for Q-0 and cyt c, respectively) we have observed saturation of the magnitude (Figs. S3 and S4). The electron transfer in RC is unidirectional that is from primary donor to terminal acceptor. The observation of cathodic current indicates that the electron transfer is taking place from electrode to RC, which is contributed by only those RCs having their primary donor side facing the electrode (den Hollander et al., 2011; Trammell et al., 2006). The large difference in magnitude of photocurrent for forward- and reverse-dipped LB films show that the majority of RC-LH1 complexes for forward-dipped films are attached to the electrode with their primary donor side facing the electrode, whereas for reverse-dipped films, only a small fraction of molecules have this particular orientation.

### 3. Current–voltage ( $I$ – $V$ ) characteristics of LB films

The detection of photocurrent gives an indication of two different orientations of RC-LH1 complexes on the electrode. This structure was further investigated using conductive atomic force microscopy (C-AFM).  $I$ – $V$  curves were recorded by sandwiching the oriented LB films between a gold electrode and a gold-coated AFM tip. A potential ramp was applied between the tip and the electrode to record the resulting current. Asymmetric  $I$ – $V$  curves were recorded for both forward- and reverse-dipped films (see Fig. S5). For forward-dipped films, more current was recorded for positively applied potential compared to negative potential whereas opposite  $I$ – $V$  curves were recorded for reverse-dipped film, that is, more current for negative potential compared to positive was recorded. RC-LH1 complex has two types of co-factors; the central part (RC complex) has a dimer of bacteriochlorophyll and two symmetric branches of co-factors, each branch containing bacteriochlorophyll, a bacteriopheophytin and quinone. The RC complex reported to have diode like  $I$ – $V$  characteristics (Lee et al., 1997; Mikayama et al., 2009, 2006; Reiss et al., 2007; Stamouli et al., 2004). The peripheral part expected to have symmetric  $I$ – $V$  response because it has similar architecture of co-factors to that of light harvesting 2 (LH2) complexes and LH2 complexes exhibit symmetric  $I$ – $V$  response across  $V=0$  (Stamouli et al., 2004). The symmetric behavior of the  $I$ – $V$  curves is attributed to the presence of carotenoid molecules, which act as molecular wires spanning the LH2 complex and they are capable of efficient electron transfer (Stamouli et al., 2004; Sumino et al., 2013).

The characteristic  $I$ – $V$  curves of RC-LH1 complexes measured in our experiments seem to have signature of both RC and LH1 complexes. The  $I$ – $V$  curves can be imagined as superimposition of a diode like  $I$ – $V$  curve and a symmetric curve across  $V=0$ . The asymmetry of  $I$ – $V$  curves arise from the presence of RC complex at the center of the LH1 ring, and the symmetric part is contributed by LH1 complex. Because the RC complex is protruding from cytoplasmic side of the membrane, the  $I$ – $V$  curves are recorded at least at an applied force of  $2$  nN, which is presumably sufficient to induce some deformation to the protruding part of RC to get access

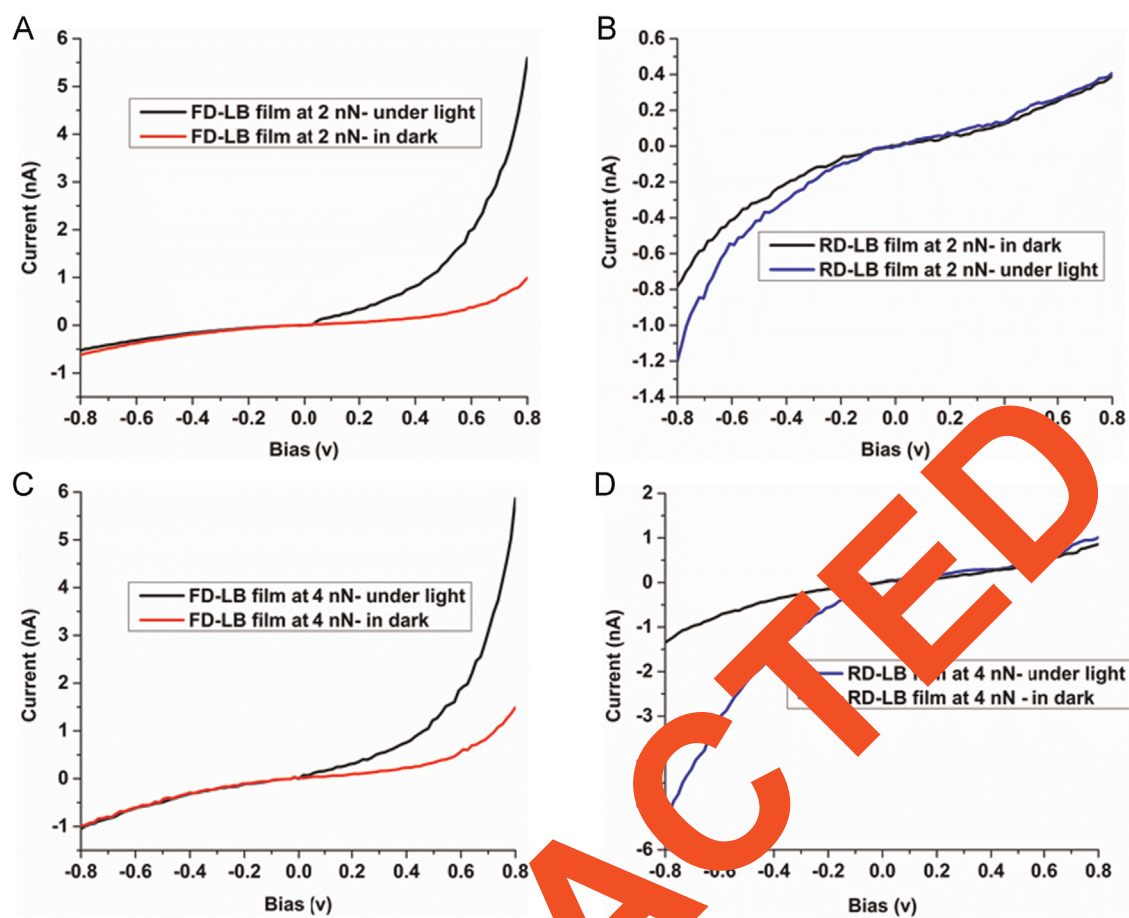


**Fig. 3.** Current–voltage ( $I$ – $V$ ) spectroscopy of forward-dipped (FD) and reverse-dipped (RD) Langmuir–Blodgett (LB) films in dark and under light illumination at different contact forces. The tunneling junction was constructed by sandwiching the oriented monolayers between a gold electrode and a gold coated AFM cantilever. The LB film was scanned by tapping mode AFM, subsequently the tip was placed at desired position and the instrument was switched to contact mode. A potential ramp was applied between the tip and electrode and resulting current was measured. (A)  $I$ – $V$  spectroscopy of FD–LB film at contact force of 2 nN in dark (red curve) and under light (black curve) conditions. (B)  $I$ – $V$  spectroscopy of RD–LB film at a contact force of 2 nN in dark (black curve) and under light (blue curve) conditions. (C)  $I$ – $V$  spectroscopy of FD–LB film at contact force of 4 nN in dark (red curve) and under light (black curve) conditions. (D)  $I$ – $V$  spectroscopy of RD–LB film at a contact force of 4 nN in dark (black curve) and light (blue curve) conditions. (For interpretation of the references to color in this figure legend, the reader is referred to the web version of this article.)

to co-factors of LH1 complex. The appearance of the contribution on opposite side of the curves for forward- and reverse-dipped films is a clear evidence of opposite orientation of films.

We have recorded  $I$ – $V$  curves at multiple points in LB films. 100  $I$ – $V$  was recorded for each sample to confirm reproducibility of the results. For forward-dipped films 80 percent of the curves represent the RC-LH1 complexes with their primary donor side facing the electrode. For reverse-dipped films, 75 percent of the  $I$ – $V$  curves show the acceptor side facing the electrode.

$I$ – $V$  curves were also acquired under light illumination. At a contact force of 2 nN the tunneling current in the  $I$ – $V$  curves of both types of films was increased but for forward-dipped LB film the increase was more pronounced than that of reverse-dipped film, quantitatively, 6 fold increase in the magnitude of current was observed for forward-dipped film compared to only 50% increase in reverse-dipped film (see Figs. 3A and B). The enhancement of the current was restricted to only part of the  $I$ – $V$  curve associated with RC, the other part of the curves (presumably contributed by LH1 ring) was unaffected by the light illumination. Different electron transfer rates for different orientations of RC complex have been previously reported. Trammell et al. for example, have measured light induced electron transfer of reaction center complex tethered to carbon electrode in two different orientations (Trammell et al., 2006). They have shown that the electron transfer rate was an order of magnitude higher when primary donor side was connected to electrode compared to the

configuration where RC was connected to the electrode via H subunit. The observed difference was attributed to different lengths of linker molecules and thickness of H subunit, which introduces an additional tunneling distance of 2.4 nm (Trammell et al., 2006). However, in our study no linker molecule is involved, so the difference in electron transfer rate can be attributed to H subunit and direct interaction of primary donor side and H subunit with the gold electrode. It was interesting to notice that by increasing the contact force, the difference in electron transfer rate in forward and reverse dipped films was decreased. At a contact force of 4 nN (see Figs. 3C and D), the current enhancement for both types of films was very similar. Hence, this force might be enough to induce sufficient deformation to H subunit to reduce the tunneling distance significantly. Therefore, we need to exert at least a force of 4 nN for RC-LH1 complexes attached to the electrode with H subunit facing the electrode to get similar electron transfer rate to that of RC-LH1 with primary electrode donor side facing the electrode. These results have unveiled new feature of RC-LH1 films that is their functional integrity under dried form. This will open new doors for applications of this protein complex in solid state electronic devices.

#### 4. Conclusions

We have been able to control the orientation of RC-LH1 complexes on a bare gold electrode. RC-LH1 complexes attached to the

electrode with their primary donor side facing the electrode resulted in faster electron transfer compared to opposite orientation. This optimized orientation of protein complexes is achieved by Langmuir–Blodgett method, a very simple deposition technique, without any modification to protein or electrode surface. *I*–*V* spectroscopy has independently verified the opposite orientations of forward- and reverse-dipped LB films. *I*–*V* curves under light illumination also showed faster electron transfer for forward-dipped LB film at low contact force. Future work will focus on contact force dependent electron tunneling in LB films, optimization of surface coverage and stability of LB films under continuous light illumination, which are important prerequisites for photovoltaic applications.

## Acknowledgments

We are thankful to Professor Thomas Schmidt (Leiden University) for letting us use the Langmuir–Blodgett trough. Professor Thijs Aartsma (Leiden University) and Dr. Raoul Frese (Free University, Amsterdam) are gratefully acknowledged for providing access to lab facilities.

## Appendix A. Supplementary information

Supplementary data associated with this article can be found in the online version at <http://dx.doi.org/10.1016/j.bios.2015.01.063>.

## References

- Akkilic, N., Kamran, M., Stan, R., Sanghamitra, N.J., 2014. *Biosens. Bioelectron.* <http://dx.doi.org/10.1016/j.bios.2014.07.051>.
- Alegria, G., Dutton, P.L., 1991a. *Biochim. Biophys. Acta* 1057, 239–244.
- Alegria, G., Dutton, P.L., 1991b. *Biochim. Biophys. Acta* 1057, 245–272.
- Cogdell, R.J., Durant, I., Valentine, J., Lindsay, J.G., Schmidt, T., 1983. *Biochim. Biophys. Acta* 722, 427–435.
- Das, R., Kiley, P.J., Segal, M., Norville, J., Yu, A.A., Wang, J., Trammell, S.A., Reddick, L.E., Kumar, R., Stellacci, F., Lebedev, N., Schnur, J., Bruce, B.D., Zhang, S.G., Baldo, M., 2004. *Nano Lett.* 4, 1079–1083.
- den Hollander, M.J., Magis, J.G., Fuchsenger, T., Aartsma, T.J., Jones, M.R., Frese, R.N., 2011. *Langmuir* 27, 10282–10294.
- Facci, P., Erokhin, V., Paddeu, S., Nicolini, L., 1998. *Langmuir* 14, 193–198.
- Fang, J.Y., Gaul, D.F., Chumanov, G., Cotton, T.M., Uphaus, R.A., 1995. *Langmuir* 11, 4366–4370.
- Fukuda, K., Shibasaki, Y., Nakahara, K., Takahashi, H., Tamura, S., Kawabata, Y., 1992. *Thin Solid Films* 210, 377–389.
- Kamran, M., Delgado, J.D., Frese, R.N., Aartsma, T.J., Frese, R.N., 2014. *Biomacromolecules* 15, 2833–2837.
- Katz, E., Willner, I., 2003. *Electroanalysis* 15, 91–947.
- Kim, S.U., Yagati, A.K., 2010. *J. Mater. Sci. Mater. Med.* 21, 1293–1298.
- Kondo, M., Iida, K., Dewa, T., Nagashima, S., Nagashima, K.V., Shimada, K., Hashimoto, H., Gardiner, A.T., Cogdell, R.J., Nango, M., 2012. *Biomacromolecules* 13, 432–438.
- Kothe, T., Poller, S., Zhao, F.Y., Fortgang, P., Rogner, M., Schuhmann, W., Plumere, N., 2014. *Chem.—A Eur. J.* 20, 11029–11034.
- Lebedev, N., Trammell, S.A., Spano, A., Lukashev, E., Griva, I., Schnur, J., 2006. *J. Am. Chem. Soc.* 128, 12044–12045.
- Lee, I., Lee, J.W., Greenbaum, E., 1997. *Phys. Rev. Lett.* 79, 3294–3297.
- Liljeroth, P., 2012. *Nat. Nanotechnol.* 7, 5–6.
- Liu, Z.F., Morigaki, K., Hashimoto, K., Fujishima, A., 1992. *Anal. Chem.* 64, 134–137.
- Mershin, A., Matsumoto, K., Kaiser, L., Yu, D.Y., Vaughn, M., Nazeeruddin, M.K., Bruce, B.D., Graetzel, M., Zhang, S.G., 2012. *Sci. Rep.* 2.
- Mikayama, T., Iida, K., Suemori, Y., Dewa, T., Miyashita, T., Nango, M., Gardiner, A.T., Cogdell, R.J., 2009. *J. Nanosci. Nanotechnol.* 9, 97–107.
- Mikayama, T., Miyashita, T., Iida, K., Suemori, Y., Nango, M., 2006. *Mol. Cryst. Liq. Cryst.* 445, 291–296.
- Mirvakili, S.M., Slota, J.E., Usagocar, A.R., Mahmoudzadeh, A., Jun, D., Mirvakili, M.N., Beatty, J.T., Madden, J.D.W., 2014. *Adv. Funct. Mater.* 24, 4789–4794.
- Nguyen, K., Bruce, B.D., 2014. *Biochim. Biophys. Bioenerg.* 1837, 1553–1566.
- Reiss, B.D., Hanson, D.K., Firestone, M.A., 2007. *Biotechnol. Prog.* 23, 985–989.
- Roszak, A.W., Howard, T.D., Southall, J., Gao, M., Law, C.J., Isaacs, N.W., Cogdell, R.J., 2003. *Science* 302, 1969–1972.
- Salverda, J.M., Patil, A.V., Mizson, G., Trammell, S.A., Akkili, N., Canters, G.W., Davis, J.J., Heering, H.A., Aartsma, T.J., 2010. *Angew. Chem.* 49, 5776–5779.
- Stamouli, A., Frenken, J.W., Oostkamp, T., Cogdell, R.J., Aartsma, T.J., 2004. *FEBS Lett.* 560, 109–114.
- Sumino, A., Dewa, T., Sasahara, K., Kondoh, M., Nango, M., 2013. *J. Phys. Chem. Lett.* 4, 1087–1092.
- Swainsbury, D.J., Friel, V.M., Jones, M.R., 2014. *Biosens. Bioelectron.* 58, 172–178.
- Talham, D.R., Yamamoto, T., Mershin, A., 2008. *J. Phys. Condens. Matter*, 20.
- Tan, S.C., Crook, R.M., Jones, M.R., Welland, M.E., 2012a. *Angew. Chem.* 51, 6667–6671.
- Tan, S.C., Crook, R.M., Jones, M.R., Welland, M.E., 2012b. *ACS Nano* 6, 9103–9109.
- Tan, S.C., Crook, R.M., Jones, M.R., Welland, M.E., 2013. *Adv. Funct. Mater.* 23, 5556–5563.
- Trammell, S.A., Spano, A., Price, R., Lebedev, N., 2006. *Biosens. Bioelectron.* 21, 1023–1028.
- Trammell, S.A., Spano, A., Price, R., Lebedev, N., 2006. *Biosens. Bioelectron.* 21, 1023–1028.
- Uehara, M., Miyake, J., Fujii, T., Shirai, M., Arai, T., Yasuda, Y., Hara, M., 1998. *Supramol. Sci.* 5, 155–166.
- Uphaus, R.A., Fang, J.Y., Picorel, R., Chumanov, G., Wang, J.Y., Cotton, T.M., Seibert, J., 1997. *Photochem. Photobiol.* 65, 673–679.
- Willner, I., Katz, E., Willner, I., 2006. *Curr. Opin. Biotechnol.* 17, 589–596.
- Willner, I., Katz, E., 2000. *Angew. Chem.* 39, 1180–1218.
- Yan, X., Faulkner, C.J., Jennings, G.K., Cliffl, D.E., 2012. *Langmuir* 28, 15080–15086.
- Yasuda, Y., Hara, M., Miyake, J., Toyotama, H., 1997. *Jpn. J. Appl. Phys. Part 2—Lett.* 36, L577–L579.
- Yasuda, Y., Hirata, Y., Sugino, H., Kumei, M., Hara, M., Miyake, J., Fujihira, M., 1992. *Thin Solid Films* 210, 733–735.
- Yasuda, Y., Sugino, H., Toyotama, H., Hirata, Y., Hara, M., Miyake, J., 1994. *Bioelectrochem. Bioenerg.* 34, 135–139.
- Yasuda, Y., Toyotama, H., Hara, M., Miyake, J., 1998. *Thin Solid Films* 327, 800–803.
- Yehezkel, O., Tel-Vered, R., Michaeli, D., Willner, I., Nechushtai, R., 2014. *Photosynth.* 120, 71–85.
- Yehezkel, O., Tel-Vered, R., Wasserman, J., Trifonov, A., Michaeli, D., Nechushtai, R., Willner, I., 2012. *Nat. Commun.* 3, 742. <http://dx.doi.org/10.1038/ncomms1741>.
- Zaitsev, S.Y., Kalabina, N.A., Zubov, V.P., Lukashev, E.P., Kononenko, A.A., Uphaus, R.A., 1992. *Thin Solid Films* 210, 723–725.
- Zhao, Y.Y., Gao, M.L., Ren, Y.Z., Dong, Z.J., Wang, H., Liu, W., Li, T.J., 1992. *Thin Solid Films* 210, 610–613.